Optical properties of strontium monochalcogenides from first principles

M. Dadsetani*
Physics Department, University of Isfahan, Isfahan, Iran
and Physics Department, Lorestan University, Lorestan, Iran

A. Pourghazi
Physics Department, University of Isfahan, Isfahan, Iran
(Received 4 November 2005; revised manuscript received 10 January 2006; published 1 May 2006)

Optical properties of strontium monochalcogenide compounds SrX (X=Se, Se, and Te) in NaCl crystal structure are calculated using the band structure results obtained through the full potential linearized augmented plane wave method. The exchange-correlation potential is treated by the generalized gradient approximation (GGA) within the scheme of J. P. Perdew, K. Burke, and M. Ernzerhof [Phys. Rev. Lett. **77**, 3865 (1996)]. Also we have used Engel and Vosko GGA formalism [E. Engel and S. H. Vosko, Phys. Rev. B. **47**, 13164 (1993)] to improve the band gap results. The real and imaginary parts of the dielectric function $\varepsilon(\omega)$, the optical absorption coefficient $I(\omega)$, the reflectivity $R(\omega)$ and the energy loss function are calculated. The calculated results show good agreement with the available experimental results, particularly in the low energy region of the spectra. Furthermore, the interband transitions responsible for the structures in the spectra are specified. It is shown that the chalcogen p states and Sr $4d$ states play the major role in optical transitions as initial and final states, respectively. The effect of the spin-orbit coupling on the optical properties is also investigated and found to be quite small, especially in the low energy region.

DOI: 10.1103/PhysRevB.73.195102 PACS number(s): 71.15.−m

I. INTRODUCTION

The strontium chalcogenides SrX (X=S, Se and Te), together with other alkaline earth chalcogenides form a very important closed shell ionic system with NaCl crystal structure at normal conditions. They are technologically important materials, with applications in the area of luminescent devices, radiation dosimetry, fast high-resolution optically stimulated luminescence imaging, and infrared sensitive devices.[1–3] These compounds form a closed shell ionic system crystallizing in the NaCl structure at normal conditions. Under higher pressure prior to metallization, they undergo a first order structural phase transition to CsCl structure.[4]

The available experimental results on the reflectivity and absorption of SrX compounds are mostly limited to the excitonic transitions.[5–9] In the optical frequency range, Kaneko and Morimoto[10,11] have measured the reflectivity and imaginary part of the dielectric function for SrSe and SrS. But for SrTe, to our knowledge, there are not yet any experimental results on these quantities in the optical frequency range. Our calculated results could serve as a reference for future experimental work on this compound.

There are a number of theoretical works on these materials concerning electronic band structure, structural phase stability, elastic properties and the metallization process.[4,5,12–19] For the band gap results, there are some discrepancies between different calculations. For example, the band gap of SrSe is predicted to be direct by Pandey, Lepak, and Jaffe,[16] and indirect by Marinelli, Dupin, and Lichanot.[13]

Considering the optical properties, to our knowledge there are only two reports, one an *ab initio* calculation of only $\varepsilon_1(0)$ for crystals with NaCl crystal structure including the SrX compounds, using the time dependent density functional approach;[20] the other one, a calculation of the imaginary part of the dielectric function only for SrS, using the linear combination of atomic orbitals (LCAO) method (within local density approximation).[21] Moreover, it seems that there is a lack of both experimental as well as theoretical data on the optical properties of strontium monochalcogenides.

In this work, we have investigated the full range of the optical properties of strontium chalcogenides including real and imaginary parts of the dielectric function, reflectivity, absorption coefficient and energy loss function using the full potential linearized augmented plane wave (FP-LAPW) method with generalized gradient approximation (GGA) for the exchange correlation potential, within the density functional theory (DFT).

A brief description of the calculation method is given in Sec. II. In Sec. III we have given the detailed band structure of SrX compounds which is needed for optical studies. The optical properties through the study of the imaginary and real parts of the dielectric function and the absorption and reflectivity spectra are discussed in Sec. IV. A brief summary and the conclusions are given in Sec. V.

II. CALCULATION METHOD

The calculations presented in this work were performed using the FP-LAPW method. In this method no shape approximation on the potential or on the electronic charge density is made. The calculations of the electronic and optical properties have been done relativistically with and without the spin-orbit coupling. We use the WIEN2K[22] implementation of the method which allows the inclusion of local orbitals in the basis, improving upon linearization and making possible a consistent treatment of the semicore and valance states in

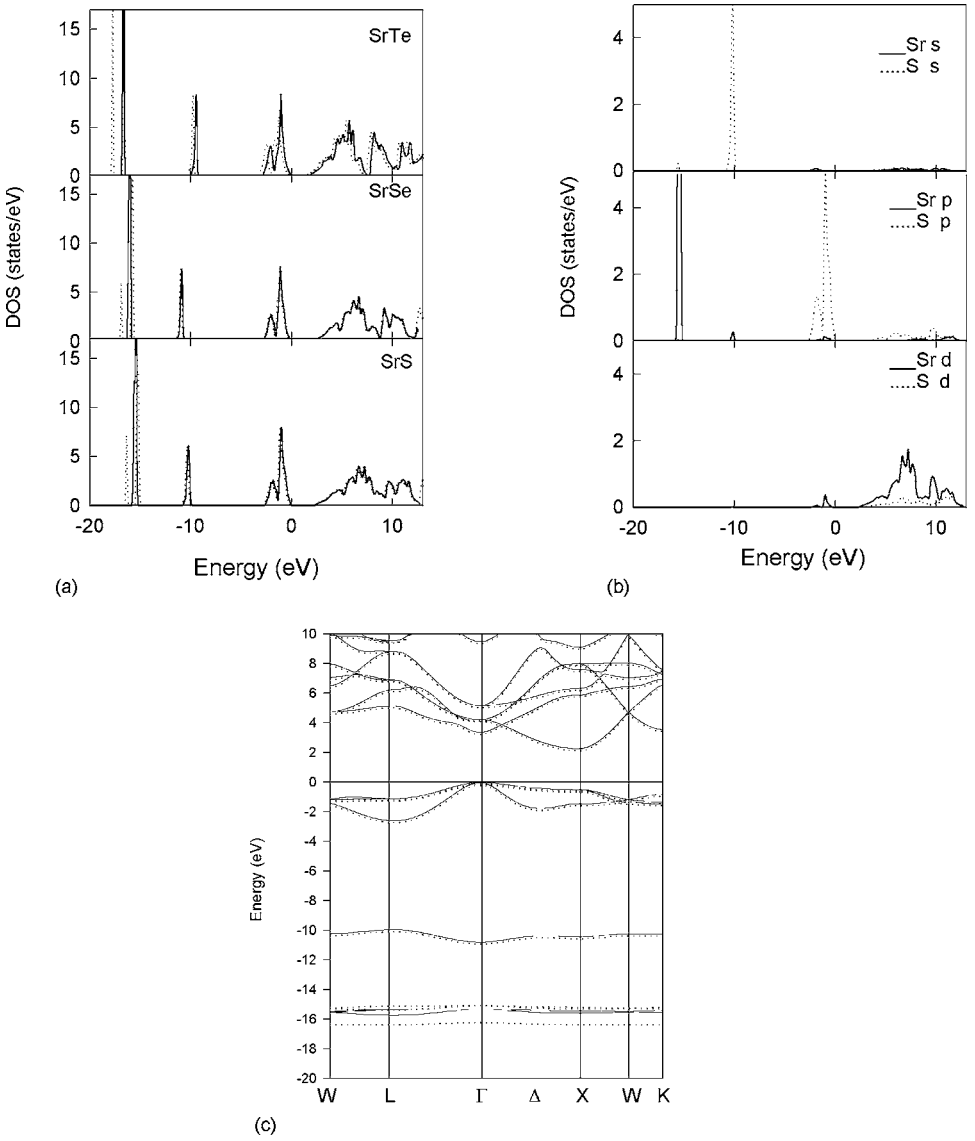

FIG. 1. (a) Total density of states with (dotted line) and without (solid line) spin-orbit coupling for all three compounds; (b) partial density of states without spin-orbit coupling for SrS; (c) electronic band structure with (dotted line) and without (solid line) spin-orbit coupling for SrS.

an energy window, hence ensuring proper orthogonality. The exchange correlation potential within the GGA is calculated using the scheme of Perdew, Burke, and Ernzerhof.[23] To calculate the band gap in addition to that the Engel and Vosko scheme[24] was applied. The convergence parameter $RK_{\max}$, which controls the size of the basis sets in these calculations, was set to 10. The $G_{\max}$ parameter was taken to be 14.0 bohr^{-1}. We have used the experimental values of the lattice parameters.[4,25,26] Brillouin-zone (BZ) integrations within the self-consistency cycles were performed via a tetrahedron method,[27] using 72 K points in the irreducible BZ. But for the calculation of the optical properties (for the imaginary part of the dielectric tensor) a denser sampling of the BZ was needed, where we used 816 K points. The muffin-tin radius was taken as 2.5 a.u. for all of four elements. All these values have been chosen in a way to ensure the convergence of the results.

III. ELECTRONIC STRUCTURE RESULTS

Our calculated total density of states (DOS) for SrTe, SrSe and SrS are given in part (a) of Fig. 1. Due to the close similarity between the results obtained for these SrX compounds, in parts (b) and (c) the partial DOS and the electronic band structure are given only for SrS. The results are given both with and without the spin-orbit coupling. The major contributions to the occupied part of the DOS come from the Sr $4p$ and $4d$ and the chalcogen s and p states.

The first structure in the low lying energy side of the DOS consists of a narrow peak centered on −16.8 eV for SrTe, −16.0 eV for SrSe and −15.5 eV for SrS. This structure originates from Sr $4p$ and corresponds to the first three lowest lying (overlapping) bands in Fig. 1. These three bands are lower in energy for SrSe and SrTe than SrS by around 0.52 eV and 1.30 eV, respectively. The structure of the spin-orbit splitting and its amount (nearly 1.0 eV) are considerable in this region. Spin-orbit coupling removes the degeneracy between two of the three bands.

The next structure, which in the absence of spin-orbit coupling is separated from the first, by a gap of 6.8 eV for SrTe, and 4.50 eV for SrSe and SrS, is a peak around 9 eV for SrTe, 11 eV for SrSe and 10 eV for SrS, below the Fermi level, and consists predominantly of chalcogen s states. This peak is highest in SrTe and smallest in SrS and corresponds

TABLE I. The calculated and experimental band gaps, E_g (eV).

	Present work							
	GGA[a]		GGA[b]		LMTO[c]	LAPW[d]	APW[e]	Exp[f]
	without so	with so	without so	with so				
SrTe	1.71	1.38	2.38	2.05	1.64		1.54	
SrSe	2.12	2.01	2.95	2.81	2.13		2.34	3.81
SrS	2.25	2.16	3.31	3.20	2.56	2.3	2.66	4.32

[a]Reference 23.
[b]Reference 24.
[c]Reference 30.
[d]Reference 31.
[e]Reference 19.
[f]Reference 6.

to the next lowest lying band shown in the band structures in Fig. 1. This band is lower in energy for SrSe and SrS than SrTe by around 120 and 0.67 eV, respectively. From the band structures we also see that the width of this peak originates from the dispersion in the region near L and Γ points in BZ. Spin-orbit coupling has a minor effect on the structure of this peak, shifting it down in energy by a very small amount.

The broader structure that is situated between −3.0 eV and the Fermi level corresponds to the three valence bands in Fig. 1. From the partial DOS, it is seen that just below the Fermi level the bands are dominated by the chalcogen p states. In the absence of spin-orbit coupling there is a triple degeneracy at Γ point and a double degeneracy at X point. Spin-orbit coupling removes the degeneracy at these points. The amount of the spin-orbit splitting is 0.84 eV, 0.40 eV, 0.11 eV at Γ point and 0.45 eV, 0.25 eV, 0.09 eV at X point for SrTe, SrSe and SrS, respectively. This splitting may be used to interpret separations between doublet excitonic excitations which was measured by others.[5,11]

The structure above the Fermi level, extending up to around 15 eV, contains a broad peak at around 5 eV for SrTe and 7 eV for SrSe and SrS, and consists mostly of Sr 4d states together with very small contributions from chalcogen p and d states.

In all three compounds we have found an indirect band gap between the top of chalcogen valence p bands occurring at the Γ point and the bottom of the Sr 4d bands occurring at the X point, confirming the previously found results by Syassen *et al.*,[5] Khenata *et al.*[12] and Hasegawa and Yanase,[19] and in contradiction to the results obtained by others.[13,15,16] The spin-orbit coupling reduces the band gap; similar results have been found for HgI_2 and SnI_2.[28,29] This reduction is bigger for SrTe than the other two compounds. The calculated values of the band gap are compared with the experimental and other calculated results in Table I. Our results are in fair agreement with the previous studies.[30,31] The small difference in the band gap between our result and another FP-LAPW result[12] is due to the difference in the lattice parameter used in the two calculations.

The results presented in Table I confirm the well known expectation that the theoretical band gaps are on the whole underestimated within GGA, in comparison with the experimental values. The major shortcoming in the DFT to calculate the energy gap roots is in the exchange correlation term that cannot be handled accurately in this method. Engel and Vosko[24] constructed a new functional form of the GGA which proved to improve the results for quantities that depend on the energy eigenvalues, including the band gap.[32] By using Engel and Vosko's generalized gradient approximation, we were able to improve our band gap results as shown in Table I.

It can be seen that the calculated energy gap values decrease with the increase of the size of the chalcogen atom. Similar behavior was observed in Ca and Ba chalcogenides.[33,34]

IV. OPTICAL PROPERTIES

The optical properties of matter can be described by means of the transverse dielectric function $\varepsilon(\omega)$. There are two contributions to $\varepsilon(\omega)$, namely, intraband and interband transitions. The contribution from intraband transitions is important only for metals. The interband transitions can further be split into direct and indirect transitions. Here we neglect the indirect interband transitions which involve scattering of phonons and are expected to give only a small contribution to $\varepsilon(\omega)$.[35] To calculate the direct interband contribution to the imaginary part of the dielectric function $\varepsilon_2(\omega)$, one must sum up all possible transitions from the occupied to the unoccupied states. Taking the appropriate transition matrix elements into account, the imaginary part of the dielectric function $\varepsilon_2(\omega)$ is given by

$$\varepsilon_2(\omega) = \frac{Ve^2}{2\pi\hbar m^2\omega^2}\int d^3k \sum_{nn'} |\langle \mathbf{k}n|\mathbf{p}|\mathbf{k}n'\rangle|^2 f(\mathbf{k}n) \times [1 - f(\mathbf{k}n')]\delta(E_{\mathbf{k}n} - E_{\mathbf{k}n'} - \hbar\omega), \quad (1)$$

where $\hbar\omega$ is the energy of the incident photon, p is the momentum operator $\frac{\hbar}{i}\frac{\partial}{\partial x}$, $|kn\rangle$ is the eigenfunction with eigenvalue E_{kn}, and $f(kn)$ is the Fermi distribution function. The evaluation of the matrix elements of the momentum operator in Eq. (1) is performed over the muffin-tin and the interstitial regions separately. A full detailed description of the calculation of these matrix elements is given by Ambrosch-Draxl and Sofo[36]

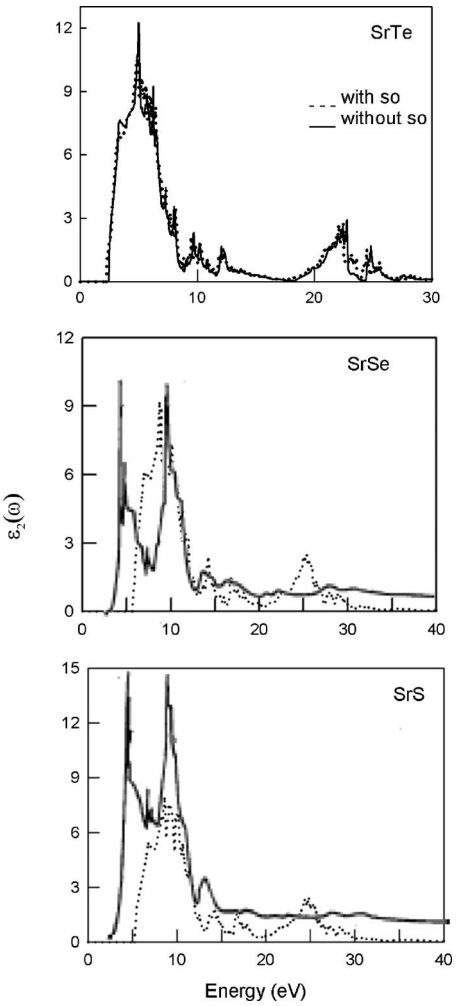

FIG. 2. Top panel: Calculated imaginary part of dielectric function for SrTe. middle panel: calculated imaginary part of dielectric function with spin-orbit coupling (dotted line) along with the experimental (solid line) for SrSe. Bottom panel: calculated imaginary part of dielectric function with spin-orbit coupling (dotted line) along with the experimental (solid line) for SrS.

The real part of the dielectric function $\varepsilon_1(\omega)$ follows from the Kramers-Kronig relation.[37]

$$\varepsilon_1(\omega) = 1 + \frac{2}{\pi}\int_0^\infty \frac{\varepsilon_2(\omega')\omega' d\omega'}{\omega'^2 - \omega^2}. \quad (2)$$

In order to calculate $\varepsilon_1(\omega)$, one needs to have a good representation of $\varepsilon_2(\omega)$ up to high energies. In the present work we have calculated $\varepsilon_2(\omega)$ up to 95 eV and have used this value as the truncation energy in Eq. (2). This energy range was chosen so as to produce convergence in the Kramers-Kronig transformation.

Our calculated imaginary parts of the dielectric function for the three compounds in the presence of the spin-orbit coupling, together with the available experimental results (for SrSe and SrS by Kaneko, Morimoto and Koda[11]) are shown in Fig. 2. The results obtained in the absence of spin-orbit coupling are only given for SrTe.

The behavior of $\varepsilon_2(\omega)$ is rather similar for all three compounds with some differences in details. The calculated $\varepsilon_2(\omega)$ has major peaks, labeled (a)–(e) in the figure. We note that all the structures in the imaginary part of dielectric function [except the peak (e)] are shifted toward lower energies as we go from S to Te. This trend may be directly inferred from the band structure results, considering the shift in the location of the first structure above the Fermi level in DOS curves, toward lower energies as we go from S to Te. The reverse trend for peak (e) is due to the shift in the first lowest structure in DOS toward lower energies as we go from S to Te.

It is worthwhile to attempt to identify the transitions that are responsible for the structures in $\varepsilon_2(\omega)$ using our calculated band structures. The locations of the peaks in $\varepsilon_2(\omega)$ together with the dominant contributions from interband transitions to each peak are given in Table II. It is obvious that the chalcogen p states and Sr $4d$ states play the major role in these optical transitions as initial and final states, respectively. Spin-orbit coupling does not have any significant effect on the result. This is to be expected, since spin-orbit coupling changes the eigenvalues only by around 0.1 eV, which is not significant in the calculation of the optical properties. This has also been found in other FP-LAPW or full potential linearized muffin-tin orbital (FP-LMTO) calculations for WSe_2 and HgI_2.[28,38]

In order to compensate the GGA underestimation of the band gap, the calculated spectra have been scissors shifted by an amount equal to the difference between the calculated and the experimental band gaps (1.80 eV for SrSe and 2.16 eV for SrS). As can be seen in the figure there is a close match between our calculated results and the experiment in the low energy region (5–17 eV), especially for SrSe. For higher energies considering the overall features of the spectra and the amplitudes, there is a reasonable agreement between the two curves, but the locations of the peaks do not coincide. Comparing to $\varepsilon_2(\omega)$ calculated for SrS by Ching, Gan and Huang,[21] not only have we obtained the results for the full experimental range, but we have also been able to reproduce the small peak occurring experimentally at around 14 eV and some other small structures, which are missing in their result.

The results for the dispersive part of the dielectric function, $\varepsilon_1(\omega)$, for the three strontium chalcogenides are given in Fig. 3. The main features in these curves are: a peak at around 3 eV; a rather steep decrease between 4 and 7 eV, after which $\varepsilon_1(\omega)$ becomes negative; a minimum, followed by a slow increase toward zero; another minimum at around 23 eV; and then again a slow increase toward zero at higher energies.

The extinction coefficient $k(\omega)$ and energy loss function $L(\omega)$ have been calculated for all three compounds. The results are quite similar, thus we have given these curves only for SrS in Fig. 4. The local maxima of the extinction coefficient, $k(\omega)$, correspond to the zeroes of $\varepsilon_1(\omega)$. But the energy loss spectra do not show any distinct maxima at these zeros of $\varepsilon_1(\omega)$ with energies smaller than 10 eV. The reason for this is that $\varepsilon_2(\omega)$ is still large at these energy values. In the range of 10–16 and 24–27 eV there are some large peaks in the energy loss spectra. At such high energies $\varepsilon_2(\omega)$ is small,

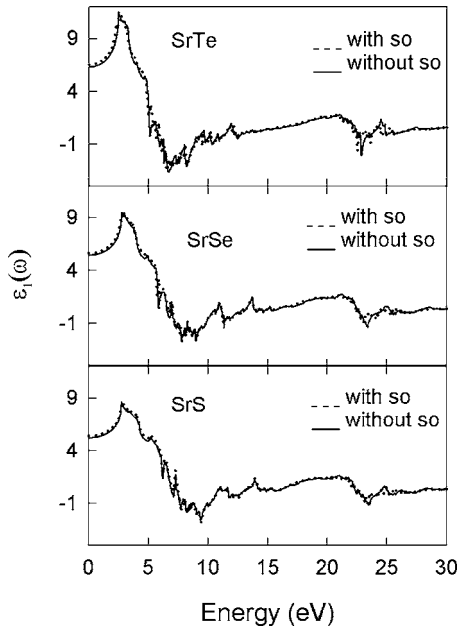

FIG. 3. Calculated real part of the dielectric function with and without spin-orbit coupling.

and thus the amplitude of the energy loss function becomes large.

In Table III our calculated dielectric constants $\varepsilon_1(0)$ are compared with the other calculations and the experimental values. Our calculated results are bigger than the experimental value, and scissors shifting improves the results substantially, but the inclusion of spin-orbit coupling increases the dielectric constant by a small amount. On the whole our scissors shifted results in the presence of spin-orbit coupling have an average deviation of about 1.6% from the experiment.

The calculated reflectivity spectra for the three compounds, together with the available experimental results (for SrSe and SrS by Kaneko, Morimoto and Koda,[11]) are given in Fig. 5, which shows the close resemblance between these compounds. The results obtained in the absence of spin-orbit coupling are only given for SrTe.

Our scissors shifted reflectivity starts at around 16% for SrS and SrSe, irrespective of whether the spin-orbit coupling is included or not; and in comparison to the experimental value, it is in good agreement for SrSe but is bigger for SrS. The experimental peaks at around 5 eV for SrSe and SrS are not present in our results. Kaneko, Morimoto and Koda[11] interpreted that the origin of these peaks are excitonic effects, which justifies their absence in our results. Our reflectivity reaches the maximum value of 50% for SrS and SrSe at around 12 eV. This closely coincides with the experimental peak which has a smaller value for both compounds.

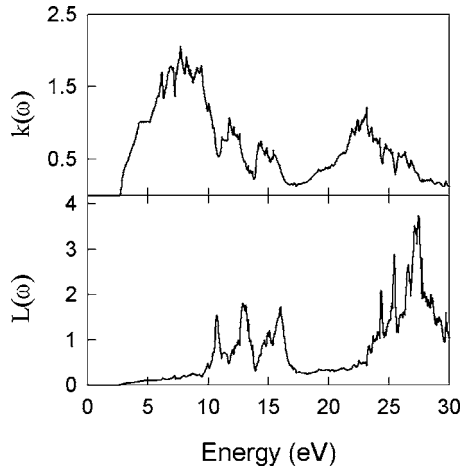

FIG. 4. Calculated extinction coefficient (top) and energy loss function (bottom) for SrS with spin-orbit coupling.

There is a dip in the reflectivity spectra at around 20 eV for both SrS and SrSe, after which the reflectivity increases and reaches some maximum value, both in our results and in the experiment. But the calculated values of the reflectivity at the dip (nearly zero) and at the maximum are not the same as the experimental values. This discrepancy is due to the broadening effects, which are not being considered in our calculations. These broadening effects are also responsible for the absence of the sharp and small (calculated) peaks in the experimental results. Considering the unreliability of the experimental results due to high chemical activity of the surface of these SrX compounds for chemical adsorption of ambient gas molecules,[11] one needs more experimental data to make any reasonable comparison in this energy range.

We have shown the calculated frequency-dependent absorption coefficient $I(\omega)$ with and without spin-orbit coupling in Fig. 6. Similar to the reflectivity spectra there are two structures present. The calculated height of the second structure is bigger than the first one, in all three compounds (with peaks at around 7 and 22 eV), and it has a minimum at around 17 eV. Spin-orbit coupling also reduces the absorption coefficient in the higher energy structure.

TABLE II. Peak positions of $\varepsilon_2(\omega)$ together with the dominant contributions to every peak.

Peak	Peak positions (eV)			The dominant transition(s)		Direct transition location in BZ
	SrTe	SrSe	SrS	from band(s)	to band	
a	3.39	4.07	4.31	6 and 7	8	K
b	4.99	5.81	6.11	7	8	L
c	9.70	11.20	11.74	7	15	$\Gamma-X$
d	12.04	13.76	14.05	7	17	$L-\Gamma$
e	22.79	22.30	22.25	1 and 3	10	W-L and X-W

TABLE III. The calculated and experimental dielectric constants.

	Present work				TDDFT[a]	OLCAO[b]	Exp[c]
	without shift		with shift				
	without so	with so	without so	with so			
SrTe	6.32	6.54			5.88		4.91
SrSe	5.46	5.64	4.18	4.26	4.77		4.33
SrS	5.20	5.37	3.96	4.03	4.37	3.68	4.09

[a]Reference 20.
[b]Reference 21.
[c]Reference 39.

V. CONCLUSIONS

We have studied the full range of the electronic and optical properties of the strontium chalcogenides SrTe, SrSe and SrS using the FP-LAPW method with and without spin-orbit coupling. The inclusion of the spin-orbit coupling reduces the band gap by about 0.33 eV for SrTe, 0.11 eV for SrSe and 0.09 eV for SrS. By using Engel and Vosko's GGA, we have performed band structure calculations and obtained better value for the band gaps, with respect to the experimental results.

The spin-orbit coupling has a very small (almost negligible) effect on the optical properties in the energy range 0–15 eV. At higher energies it has a more pronounced effect on the details of the peak positions and the average values of the calculated reflectivity and absorption coefficient. Furthermore, we have shown that the chalcogen p states and Sr $4d$ states play a major role in these optical transitions as initial and final states, respectively. Regardless of the excitonic transitions, there is a good agreement between our calculated imaginary part of the dielectric function and the reflectivity with experiment in the low energy part of the spectra, and an even better one for SrSe, which has a smaller band gap. Therefore, we predict that our results for SrTe (with a still smaller band gap) will show better agreement with the future experimental works. Our scissors shifted results of the dielectric constants in the presence of spin-orbit coupling have an average deviation of about 1.6% from the experiment.

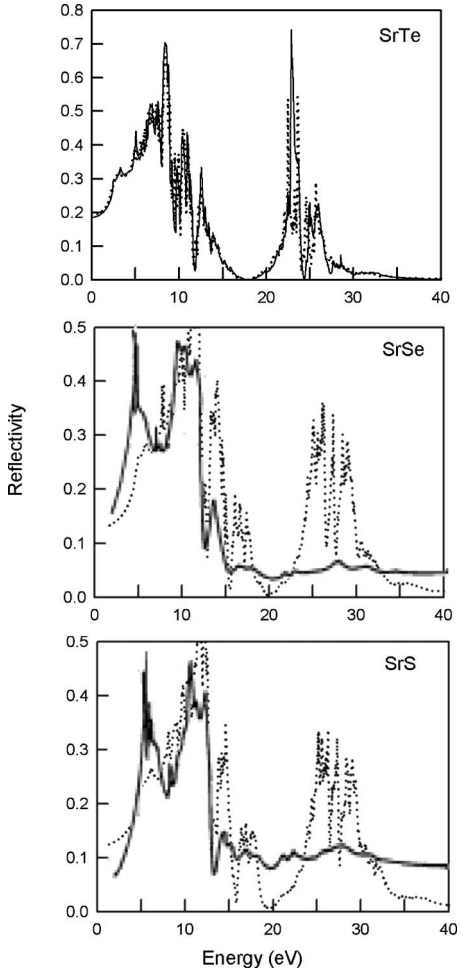

FIG. 5. Top panel: Calculated reflectivity with (dotted line) and without (solid line) spin-orbit coupling for SrTe. middle panel: calculated reflectivity with spin-orbit coupling (dotted line) along with the experimental (solid line) for SrSe. Top panel: calculated reflectivity with spin-orbit coupling (dotted line) along with the experimental (solid line) for SrS.

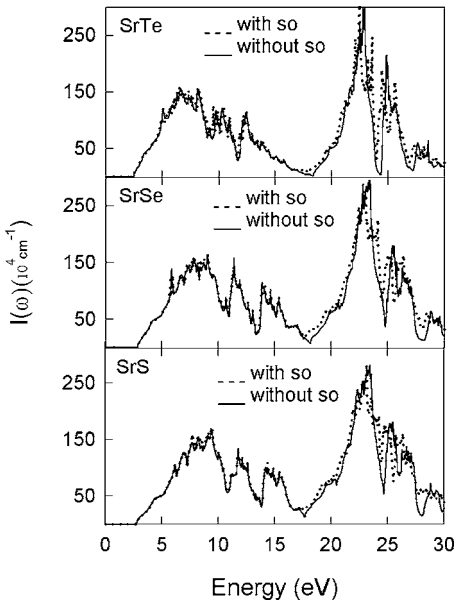

FIG. 6. Calculated absorption coefficient with and without spin-orbit coupling.

*Electronic address: dadsetani_m@yahoo.com

[1] Y. Nakanishi, T. Ito, Y. Hatanaka, and G. Shimaoka, Appl. Surf. Sci. **66**, 515 (1992).
[2] S. Asano, N. Yamashita, and Y. Nakao, Phys. Status Solidi B **89**, 663 (1978).
[3] R. Pandey and S. Sivaraman, J. Phys. Chem. Solids **52**, 211 (1991).
[4] H. Luo, R. G. Greene, and A. L. Ruoff, Phys. Rev. B **49**, 15341 (1994).
[5] K. Syassen, N. E. Christensen, H. Winzen, K. Fischer, and J. Evers, Phys. Rev. B **35**, 4052 (1987).
[6] Y. Kaneko and T. Koda, J. Cryst. Growth **86**, 72 (1988).
[7] N. Yamashita, A. Iwasaki, A. Asano, M. Ohishi, and K. Ohmari, J. Phys. Soc. Jpn. **53**, 4425 (1984).
[8] R. J. Zollweg, Phys. Rev. **111**, 113 (1958).
[9] G. A. Saum and E. B. Hensley, Phys. Rev. **113**, 1019 (1959).
[10] Y. Kaneko, K. Morimoto, and T. Koda, J. Phys. Soc. Jpn. **51**, 2247 (1982).
[11] Y. Kaneko, K. Morimoto, and T. Koda, J. Phys. Soc. Jpn. **52**, 4385 (1983).
[12] R. Khenata, H. Baltache, M. Rerat, M. Driz, M. Sahnoun, B. Bouhafs, and B. Abbar, Physica B **339**, 208 (2003).
[13] F. Marinelli, H. Dupin, and A. Lichanot, J. Phys. Chem. Solids **61**, 1707 (2000).
[14] P. K. Jha, U. K. Sakalle, and S. P. Sanyal, J. Phys. Chem. Solids **59**, 1633 (1998).
[15] R. Pandey, P. Lepak, and J. E. Jaffe, Phys. Rev. B **46**, 4976 (1992).
[16] R. Pandey, J. E. Jaffe, and A. B. Kunz, Phys. Rev. B **43**, 9228 (1991).
[17] K. Syassen, Physica B & C **139**, 277 (1986).
[18] H. G. Zimmer, H. Winzen, and K. Syassen, Phys. Rev. B **32**, 4066 (1985).
[19] A. Hasegawa and A. Yanase, J. Phys. C **13**, 1995 (1980).
[20] F. Kootstra, P. L. de Boeij, and J. G. Snijders, Phys. Rev. B **62**, 7071 (2000).
[21] W. Y. Ching, F. Gan, and M. Huang, Phys. Rev. B **52**, 1596 (1995).
[22] P. Blaha, K. Schwarz, G. K. H. Madsen, D. Kavanicka, and J. Luitz, WIEN2K, An augmented plane wave plus local orbitals program for calculating crystal properties, Vienna University of Technology, Austria, 2001.
[23] J. P. Perdew, K. Burke, and M. Ernzerhof, Phys. Rev. Lett. **77**, 3865 (1996).
[24] E. Engel and S. H. Vosko, Phys. Rev. B **47**, 13164 (1993).
[25] K. Syassen, Phys. Status Solidi A **91**, 11 (1985).
[26] H. G. Zimmer, H. Winzen, and K. Syassen, Phys. Rev. B **32**, 4066 (1985).
[27] P. E. Blochl, O. Jepsen, and O. K. Andersen, Phys. Rev. B **49**, 16223 (1994).
[28] R. Ahuja, O. Eriksson, B. Johansson, S. Auluck, and J. M. Wills, Phys. Rev. B **54**, 10419 (1996).
[29] P. Ravindran, A. Delin, R. Ahuja, B. Johansson, S. Auluck, J. M. Wills, and O. Eriksson, Phys. Rev. B **56**, 6851 (1997).
[30] I. B. Shameen Banu, M. Rajagopalan, B. Palanivel, G. Kalpana, and P. Shenbagaraman, J. Low Temp. Phys. **112**, 211 (1998).
[31] V. S. Stepanyuk, A. Szasz, O. V. Farberovich, A. A. Grigorenko, A. V. Kozlov, and V. V. Mikhailin, Phys. Status Solidi B **155**, 215 (1989).
[32] P. Dufek, P. Blaha, and K. Schwarz, Phys. Rev. B **50**, 7279 (1994).
[33] I. B. S. Banu, G. Kalpana, B. Palanivel, P. Shenbagaraman, M. Rajagopalan, and M. Yousuf, Int. J. Mod. Phys. B **12**, 1709 (1998).
[34] G. Kalpana, B. Palanivel, and M. Rajagopalan, Phys. Rev. B **50**, 12318 (1994).
[35] N. V. Smith, Phys. Rev. B **3**, 1862 (1971).
[36] C. Ambrosch-Draxl and J. O. Sofo, cond-mat/0402523 (unpublished).
[37] F. Wooten, *Optical Properties of Solids* (Academic, New York, 1972).
[38] S. Sharma, C. Ambrosch-Draxl, M. A. Khan, P. Blaha, and S. Auluck, Phys. Rev. B **60**, 8610 (1999).
[39] M. E. Lines, Phys. Rev. B **41**, 3372 (1990).